IEEE Access
Multidisciplinary | Rapid Review | Open Access Journal

Received 16 June 2023, accepted 22 June 2023, date of publication 26 June 2023, date of current version 30 June 2023.

*Digital Object Identifier 10.1109/ACCESS.2023.3289553*

RESEARCH ARTICLE

# Noise-Reduced and PVT-Robust Double-Balanced CMOS Mixer Using Common-Mode Feedback

**CHANG-WOO LIM[1], JI-YOUNG LEE[1,2], MYOUNG-GYUN KIM[1,3], AND TAE-YEOUL YUN[1], (Member, IEEE)**

[1]Department of Electronic Engineering, Hanyang University, Seoul 133-791, Republic of Korea
[2]SK Hynix Inc., Icheon, Gyeonggi-do 17336, South Korea
[3]Samsung Electronics Company Ltd., Hwaseong-si, Gyeonggi-do 16677, South Korea

Corresponding author: Tae-Yeoul Yun (taeyeoul@hanyang.ac.kr)

This work was supported by the National Research Foundation of Korea under Grant 2018R1A5A7025522.

**ABSTRACT** This paper presents a noise reduction technique using common-mode feedback in active CMOS mixers. The proposed technique decreases the common-mode noise, thus reducing the common-to-differential conversion noise arising from mismatch and process variations. In addition, the proposed technique reduces sensitivity to process, voltage, and temperature (PVT) variations due to negative feedback. A negative feedback theory is adopted to analyze the low-noise performance of the proposed technique. The theoretical analysis is validated by simulations and measurements. The conventional and proposed mixers are fabricated in a 65-nm CMOS process. Measurement results of the proposed mixer operating at an RF of 2.1 GHz show a conversion gain of 21.5 dB, the input-referred third-order intercept point (IIP3) of -16.2 dBm, and a flicker noise figure of 8.7 dB at 10 kHz while it dissipates 3.45 mW from a 1.5 V supply voltage. Measurements also show common-mode noise reduction of 10.1 dB at 10 kHz, without degradation of other characteristics. It is demonstrated that the proposed mixer can be applied to decrease phase noise of a self-oscillating mixer (SOM) due to the low common-mode flicker noise mixer.

**INDEX TERMS** CMOS mixer, common-mode feedback, flicker noise, white noise.

## I. INTRODUCTION

In wireless communication systems, a mixer following a low noise amplifier is an important building block because low-frequency ($1/f$) or flicker noise affects the noise performance of the entire system, especially in direct conversion receivers [1]. Several methods to reduce flicker noise in active CMOS mixers have been proposed [2], [3], [4], [5], [6], [7], [8], [9], [10], but these are focused narrowly on reducing differential-mode flicker noise generated by only an LO switching stage.

Differential flicker noise ($V_{\mathrm{fn,sw}}$) from the LO switching stage is caused by direct and indirect mechanisms [2]. To decrease direct-mechanism flicker noise at low dc current in the LO switching stage, a static current bleeding technique is popularly adopted [3], [4], [5], [6]. To further decrease this noise, a dynamic current bleeding technique has been proposed [7], [8] whereby current is injected only at the instants of switching to eliminate direct flicker noise caused by the LO switching stage. Resonating inductors can be employed to tune out the parasitic capacitance and thereby to decrease indirect-mechanism flicker noise [4], [9]. In addition, mutual noise cancellation has been reported [10], where flicker noise of the main mixer is cancelled using an auxiliary mixer and mutual inductance.

Common-mode flicker noise, generated from the RF transconductance ($V_{\mathrm{fn,rf}}$) and current source ($V_{\mathrm{fn,cs}}$), appears at each output equally. Common-mode flicker noise is typically much greater than the differential flicker noise ($V_{\mathrm{fn,sw}}$) because $V_{\mathrm{fn,sw}}$ is generated only at the LO switching instant, but $V_{\mathrm{fn,rf}}$ and $V_{\mathrm{fn,cs}}$ are generated throughout the whole LO period. Because the common flicker noise can be completely suppressed by a following ideal differential amplifier or balun, it is considered insignificant. In reality, however,

The associate editor coordinating the review of this manuscript and approving it for publication was Dominik Strzalka.

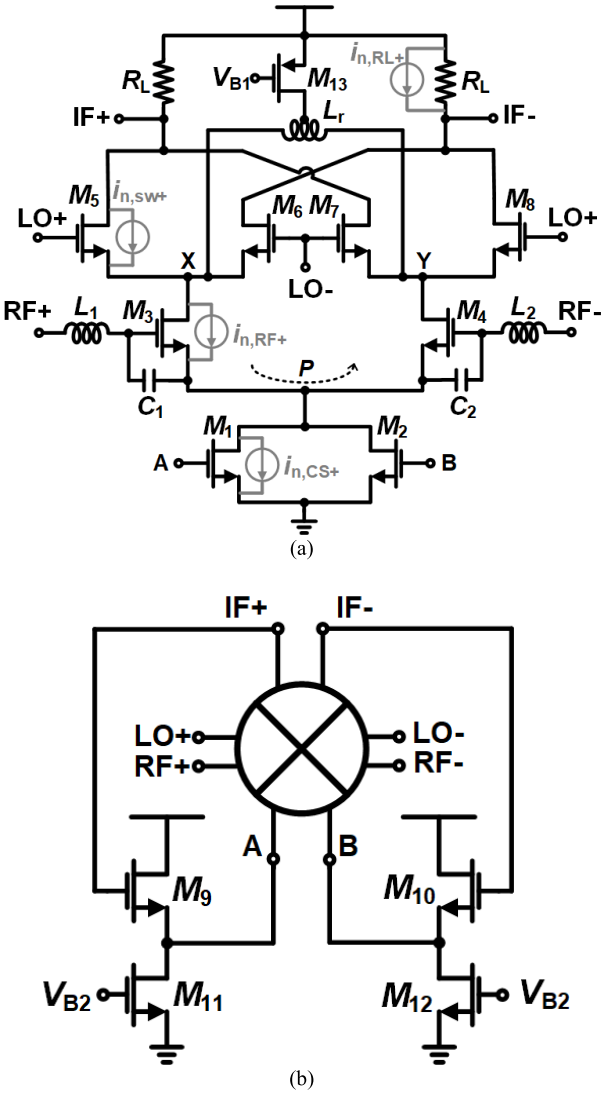


**FIGURE 1.** Schematics of (a) the conventional mixer including noise current sources and (b) the proposed common-mode feedback mixer.

mismatch and process variations cause the common flicker noise to be converted into differential flicker noise in the mixer in non-negligible amounts [11]. In addition, the mixer's common flicker noise affects the jitter and phase noise of the voltage-controlled oscillator (VCO) in VCO-integrated mixers such as the self-oscillating mixer (SOM) [12]. The common flicker noise flowing into the VCO then increases the AM-to-PM noise, thereby degrading the phase noise performance. Therefore, it is very important to reduce the common flicker noise in the mixer for high-performance transceivers.

In this paper, we propose a noise reduction technique based on common-mode feedback for use in active CMOS mixers. The common-mode feedback has been used in a mixer to stabilize the DC bias and to enhance the second-order intercept point (IP2) performance [13], not to reduce noise. The common-mode flicker and white noises caused by the tail current source, transconductance, and load stages are reduced by a simple feedback circuit, which is analyzed based on the negative feedback theory. Because a common-mode feedback path is employed between the mixer output and tail current source where only the baseband signal is handled, there is no RF signal leakage. In addition, the proposed technique does not degrade the conversion gain or linearity performance due to the 'common-mode' feedback but achieves robustness against process, voltage, and temperature (PVT) variations due to the 'negative' feedback. The common-mode feedback technique also lowers a DC offset voltage that is mainly generated from device mismatch, LO self-mixing due to finite port-to-port isolation, and even-order nonlinearity.

We have studied mixer structures similar to that discussed in the present work [14], [15], which are based on the switched biasing technique to decrease flicker noise. This technique works well when the output signal is large enough to allow alternating operation of the current source transistors between accumulation and strong inversion regions. The switched biasing technique is thus useful only when the input RF signal and conversion gain are very large. This paper is organized as follows. Section II theoretically analyzes how the proposed feedback technique decreases common-mode noise. The theoretical analysis is validated using simulation in Section III and measurement in Section IV. In Section V, we demonstrate PVT robustness and discuss common-mode noise on SOM. Finally, Section VI presents our conclusions.

## II. NOISE ANALYSIS

### A. CIRCUIT STRUCTURE

Figs. 1 (a) and (b) respectively show the conventional and proposed mixers based on the double-balanced Gilbert-cell mixer and consisted of a tail current source ($M_1$, $M_2$), a transconductance stage ($M_3$, $M_4$), a switching stage ($M_5$–$M_8$), and a load stage ($R_L$). Inductors ($L_1$, $L_2$) and capacitors ($C_1$, $C_2$) at the input port function as an input impedance matching network. In addition, a current-bleeding stage ($M_{13}$) [3], [4], [5], [6] and a resonating inductor ($L_r$) [4], [9] are adopted to decrease noise. The proposed mixer adds a source follower ($M_9$–$M_{12}$) into the conventional mixer. The source follower is utilized to form the common-mode feedback path between the mixer output and tail current source and performs the role of a DC level shifter.

The DC level shifter senses the output noise voltage that drives the tail current source and is fed back to the noise current. Meanwhile, the differential intermediate-frequency (IF) signals are not fed back because they are cancelled out at the drain of the tail current source. Therefore, the proposed technique operates as a common-mode feedback that improves common-mode noise without degrading the other mixer performances of operating frequency, conversion gain, and linearity.

It is necessary to confirm stability when the feedback technique is adopted. The dominant pole of the proposed mixer will be generated at output node because there are many

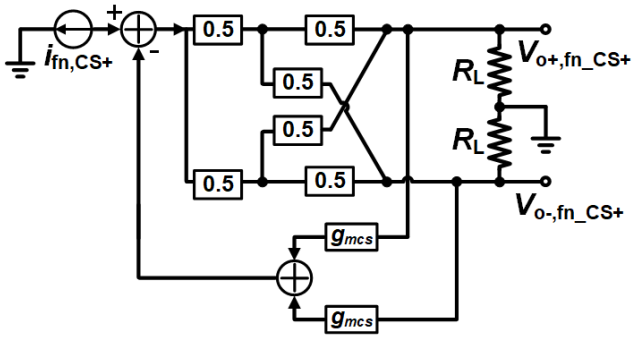


**FIGURE 2.** Common-mode feedback scheme to reduce the output flicker noise from the tail current source stage.

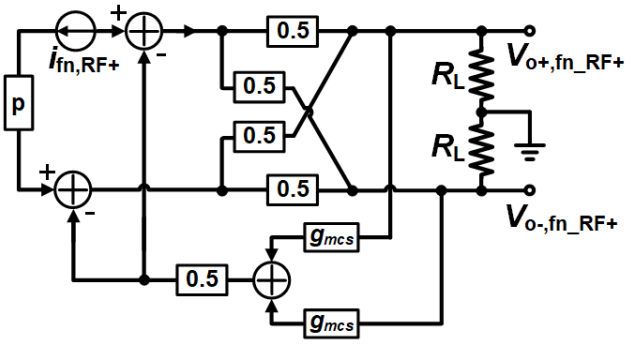


**FIGURE 3.** Common-mode feedback scheme to reduce the output flicker noise from the transconductance stage.

devices and thus many parasitic capacitances connected at output node with large $R_L$ of 1 kΩ. Therefore, devices connected to output node including the source follower should be designed carefully. The proposed mixer is designed with the phase margin of 61.62 degrees at 364.7 MHz and thus is much stable.

The common-mode feedback technique adopted in the proposed mixer decreases both flicker and white noises. Noise reductions at low and high frequencies are theoretically described in detail in Sections II-B and C, respectively. Here, low frequency refers to the frequency range in which $1/f$ noise predominates, whereas high frequency refers to the range in which white noise predominates.

As shown in Fig. 1 (a), for simplicity of analysis, we assume that four kinds of noise sources arise from the transistors ($M_1$, $M_3$, and $M_5$) and resistor ($R_L$) on one side: $i_{n,CS+}$, $i_{n,RF+}$, $i_{n,sw+}$, and $i_{n,RL+}$, respectively. Each noise current source is divided into flicker noise ($i_{fn}$) and white noise ($i_{wn}$). Because the load stage of $R_L$ does not produce flicker noise, low-frequency noise for the load stage is not considered. In addition, we ignore noises from the DC level shifter and current-bleeding stage for simplicity of analysis because their noise contributions are very small, compared to other noise sources.

### B. LOW-FREQUENCY NOISE

First, we investigate the output flicker noise generated from the tail current source and transconductance stages. In the conventional mixer, the switching transistor multiplies these noise currents by a square wave toggling between 0 and 1. Thus, the output noise currents at each output are equal to

$$i_{o+}(t) = i_n\Big(\frac{1}{2} + \frac{2}{\pi}\cos\omega_{LO}t - \frac{2}{3\pi}\cos 3\omega_{LO}t + \frac{2}{5\pi}\cos 5\omega_{LO}t - \cdots\Big) \quad (1a)$$

$$i_{o-}(t) = i_n\Big(\frac{1}{2} - \frac{2}{\pi}\cos\omega_{LO}t + \frac{2}{3\pi}\cos 3\omega_{LO}t - \frac{2}{5\pi}\cos 5\omega_{LO}t + \cdots\Big) \quad (1b)$$

where $i_n$ is the noise current generated from the tail current source and transconductance stages, and $\omega_{LO}$ is an LO frequency. The first term represents the mixing of the transferred noise current with a DC component of switching. The other terms represent mixing of the noise current with an LO fundamental frequency and its harmonics. Flicker noise generated from the current source and transconductance stages appears through a DC component of switching at each output equally, but flicker noise up-converted by switching does not occur in a desired IF range. In addition, the white noise current near the fundamental and harmonic frequencies can be down-converted to flicker noise by switching; however, these noises are neglected because the white noise from the current source and transconductance stages is much weaker than the flicker noise. Therefore, in the proposed mixer, both output flicker noises from the tail current source and transconductance stages become the in-phase or common mode and are reduced by the common-mode feedback.

The feedback topology in Fig. 1 is simplified as conceptually shown in Figs. 2 and 3, allowing only the flicker noise current source ($i_{fn\_CS+}$) from $M_1$ and the flicker noise current source ($i_{fn\_RF+}$) from $M_3$, respectively. In Figs. 1 and 2, $i_{fn\_CS+}$ is divided into $M_3$ and $M_4$ and consequently flows to the LO switching stage with a factor of 0.5 of (1). Thus, one-half of $i_{fn\_CS+}$ flows to each output equally. In Figs. 1 and 3, on the other hand, $i_{fn\_RF+}$ flows to the output ports not only directly but through route '$P$.' These noise currents are out-of-phase and thus ideally cancelled at the output. However, in reality, some of the noise current through route $P$ leaks to the tail current source stage due to the finite output resistance ($r_{o,CS}$). Therefore, noise from $i_{fn\_RF+}$ at output ports are not cancelled perfectly, and a little amount of $i_{fn\_RF+}$ is remained to each output equally. In Figs. 1, 2, and 3, the output currents from $i_{fn\_CS+}$ and $i_{fn\_RF+}$ are transferred to the output common-mode noise voltages ($V_{o\pm,fn\_CS+}$, $V_{o\pm,fn\_RF+}$) by the load resistor ($R_L$). The output noise voltage is transferred to noise current through the DC level shifter and the tail current source.

In a conventional double-balanced mixer of the open loop without the proposed feedback technique, the single output

voltage noises from $i_{\mathrm{fn\_CS+}}$ and $i_{\mathrm{fn\_RF+}}$ can be respectively expressed as

$$\overline{V_{o\pm,fn\_CS+}^2} = \left(\frac{1}{2}\right)^2 R_L^2 \cdot \overline{i_{fn,CS+}^2} \tag{2a}$$

$$\overline{V_{o\pm,fn\_RF+}^2} = (1-a)^2 \left(\frac{1}{2}\right)^2 R_L^2 \cdot \overline{i_{fn,RF+}^2} \tag{2b}$$

where

$$\overline{i_{fn,CS+}^2} = g_{mcs}^2 \overline{V_{fn,CS+}^2} \tag{2c}$$

$$\overline{i_{fn,RF+}^2} = g_{mrf,dg}^2 \overline{V_{fn,RF+}^2} \tag{2d}$$

$$g_{mrf,dg} = \frac{g_{mrf}}{1 + g_{mrf}\left(r_{o,CS}/2 \| 1/g_{mrf}\right)} \tag{2e}$$

$$a = \frac{r_{o,CS}/2}{r_{o,CS}/2 + 1/g_{mrf}}. \tag{2f}$$

Here, $g_{\mathrm{mcs}}$ and $g_{\mathrm{mrf}}$ are the transconductances of the tail current transistors ($M_1$, $M_2$) and the transconductance transistors ($M_3$, $M_4$), respectively, $g_{\mathrm{mrf,dg}}$ is the source-degenerated transconductance of the transconductance transistors ($M_3$, $M_4$), $V_{\mathrm{fn,CS+}}$ and $V_{\mathrm{fn,RF+}}$ are input-referred flicker noise voltages in the tail current source and the transconductance stages, respectively, and $a$ is the leakage ratio of $i_{f\,\mathrm{n,RF+}}$through route $P$, as depicted in Fig. 1.

In the proposed mixer, which is of closed loop form and includes the proposed feedback technique, the single output voltage noises are

$$\overline{V_{o\pm,fn\_CS+}^2} = \frac{(1/2)^2}{(1+g_{mcs}R_L)^2} R_L^2 \cdot \overline{i_{fn,CS+}^2} \tag{3a}$$

$$\overline{V_{o\pm,fn\_RF+}^2} = (1-a)^2 \frac{(1/2)^2}{(1+g_{mcs}R_L/2)^2} R_L^2 \cdot \overline{i_{fn,RF+}^2} \tag{3b}$$

Therefore, the common-mode feedback reduces the flicker noise contribution by a factor of the denominator of (3).

Second, we investigate the output flicker noise generated from the switching stage, which has been analyzed using a noise pulses model neglecting the channel length modulation effect [2]. The single output voltage noise from $i_{\mathrm{fn\_SW+}}$ is

$$\overline{V_{o\pm,fn\_sw+}^2} = R_L^2 \cdot \overline{i_{fn,sw+}^2} \tag{4a}$$

where

$$\overline{i_{fn\_sw+}^2} = \left(\frac{1}{2}\right)^2 \left(\frac{I}{\pi A} + \frac{2C_p}{T_{LO}} \cdot \frac{(C_p\omega_{LO})^2}{g_{mLO}^2 + (C_p\omega_{LO})^2}\right)^2 \times \overline{V_{fn,sw+}^2}. \tag{4b}$$

Here, $I$ is a DC current at the switching transistor, $A$ is an amplitude of the LO swing, $C_{\mathrm{p}}$ is a parasitic capacitance at the source of the switching transistors ($M_5$–$M_8$), $T_{\mathrm{LO}}$ is a time period of the LO signal, $g_{\mathrm{mLO}}$ is the transconductance of the switching transistors, and $V_{fn\_sw+}$ is an input-referred flicker noise voltage in the switching stage. The first and second terms in (4b) are the direct and indirect flicker noise, respectively. Because the output noise voltages generated from the switching stage have the out-of-phase or differential mode, these are not affected by the proposed common-mode feedback loop.

In summary, because the tail current source and RF transconductance stages consist of two transistors each, and the switching stage has four transistors, the total output voltage noise at the single output in the conventional mixer can be expressed as follows:

$$\overline{V_{o\pm,fn}^2} = \left(\frac{\overline{i_{fn,CS+}^2}}{2} + \frac{(1-a)^2 \cdot \overline{i_{fn,RF+}^2}}{2} + 4 \cdot \overline{i_{fn,sw+}^2}\right) R_L^2. \tag{5}$$

In the proposed mixer, the total output voltage noise at the single output is given by

$$\overline{V_{o\pm,fn}^2} = \left(\frac{\overline{i_{fn,CS+}^2}}{2\,(1+g_{mcs}R_L)^2} + \frac{(1-a)^2 \cdot \overline{i_{fn,RF+}^2}}{2\,(1+g_{mcs}R_L/2)^2} + 4 \cdot \overline{i_{fn,sw+}^2}\right) R_L^2 \tag{6}$$

It is evident from this equation that noise can be reduced by increasing the feedback factors $g_{mcs}$ and $R_{\mathrm{L}}$.

### C. HIGH-FREQUENCY NOISE

The proposed common-mode feedback through the tail current source reduces not only flicker noise but also white noise in an active mixer. Similar to the low-frequency noise, high-frequency noise is produced from the tail current source, transconductance, switching, and load stages.

First, the tail current source and transconductance stages generate channel noise or white noise, which is mixed with a DC component of switching and also down-converted by the LO fundamental and harmonics of switching represented by (1) [2]. Note that white noise mixed with a DC component of switching appears at each output equally and thus is reduced by the proposed common-mode feedback as well as the previous low-frequency noise analysis. Considering (1) and the mixer structure in Fig. 1, down-converted white noise from the tail current source stage is cancelled at the output, but down-converted white noise from the transconductance stage differentially appears at the outputs, which is not reduced by the common-mode feedback.

In a conventional double-balanced mixer without the proposed feedback technique, the single output white voltage noises from the current source and transconductance stages are calculated based on the above explanation to give results similar to (2):

$$\overline{V_{o\pm,wn\_CS+}^2} = \left(\frac{1}{2}\right)^2 R_L^2 \cdot \overline{i_{wn,CS+}^2} \tag{7a}$$

$$\overline{V_{o\pm,wn\_RF+}^2} = \left[(1-a)^2\left(\frac{1}{2}\right)^2 + \left(\frac{1}{2}\right)^2\left(\frac{2}{\pi}\right)^2 (1+a)^2\right] \times \cdot R_L^2 \cdot \overline{i_{wn,RF+}^2} \tag{7b}$$

where

$$\overline{i_{wn,CS+}^2} = 4kT\gamma g_{mcs} \tag{7c}$$

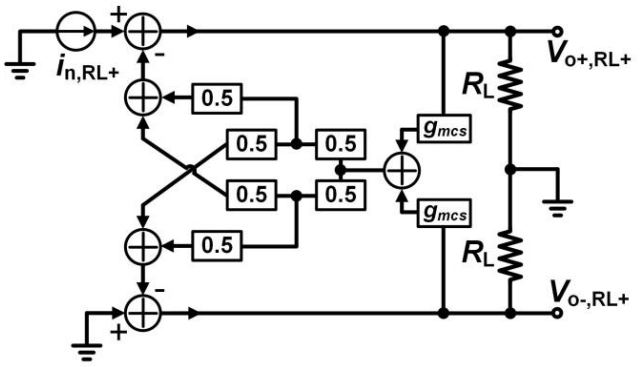


**FIGURE 4.** Common-mode feedback scheme to reduce the output white noise induced by the load resistors.

$$\overline{i^2_{wn,RF+}} = 4kT\gamma g_{mrf} \tag{7d}$$

Here, $k$ is the Boltzmann constant, $T$ is the absolute temperature, and $\gamma$ is a channel noise factor of the MOSFET. (7a) and the first term in (7b) are produced by the white noise currents ($i_{\mathrm{wn,CS+}}$, $i_{\mathrm{wn,RF+}}$) mixed with a DC component of switching. Here, both noises are common-mode noise. The second term in (7b) is produced from the down-converted white noise current, which includes effects of noise components of lower and upper sidebands at $\omega_{\mathrm{LO-IF}}$ and $\omega_{\mathrm{LO+IF}}$, respectively, and also in-phase through route $P$. The down-converted white noise current mixed with the harmonics is neglected because the white noise current ($i_{\mathrm{wn,RF+}}$) at harmonics is leaked via a parasitic capacitance, and the coefficients of harmonics in (1) are also much smaller than the fundamental value. The second term in (7b) is differential-mode noise.

In the proposed mixer, the common-mode feedback affects the output white noise mixed with only the DC component of switching, as explained above. Similar to the low-frequency noise analysis, the single output white voltage noise by the common-mode feedback is

$$\overline{V^2_{o\pm,wn\_CS+}} = \frac{(1/2)^2}{(1+g_{mcs}R_L)^2} R_L^2 \cdot \overline{i^2_{wn,CS+}} \tag{8a}$$

$$\overline{V^2_{o\pm,wn\_RF+}} = \left[ (1-a)^2 \frac{(1/2)^2}{(1+g_{mcs}R_L/2)^2} + \left(\frac{1}{2}\right)^2 \left(\frac{2}{\pi}\right)^2 (1+a)^2 \right] \cdot R_L^2 \cdot \overline{i^2_{wn,RF+}} \tag{8b}$$

The common-mode feedback differently affects flicker noise in (3) and white noise in (8). For the tail current source stage, the amount of noise reduction is the same because both noises are the common mode. Meanwhile, for the RF transconductance stage, the amount of noise reduction is very different because white noise consists of not only common-mode noise but also differential-mode noise, and the differential-mode noise is not reduced by the common-mode feedback.

Second, white noise in switching transistors has been modeled using a train of pulses, neglecting the channel length modulation effect [2], similar to the modeling of direct flicker noise for a switching transistor. The single output white voltage noise introduced by the white noise of the switching transistor is

$$\overline{V^2_{o,wn\_sw+}} = R_L^2 \cdot \overline{i^2_{wn,sw+}} \tag{9a}$$

where

$$\overline{i^2_{wn,sw+}} = kT\gamma \frac{I}{\pi A}. \tag{9b}$$

Because the output white noise generated from the switching stage is differential, similar to the low-frequency noise, it is not affected by the proposed common-mode feedback.

Third, the load stage involves only thermal noise from the resistor ($R_{\mathrm{L}}$) if active loads are not adopted. Assuming that the channel-length modulation is neglected, in the conventional mixer, the output white voltage noise from the load resistor is

$$\overline{V^2_{o+,RL+}} = R_L^2 \cdot \overline{i^2_{n,RL+}} \tag{10a}$$

$$\overline{V^2_{o-,RL+}} = 0 \tag{10b}$$

where

$$\overline{i^2_{n,RL+}} = \frac{4kT}{R_L}. \tag{10c}$$

In the proposed common-mode feedback loop, the white noise of the load resistor is fed back to the tail current source and flows through the transconductance stage. Because the down-converted white noise current is cancelled at the output port, similarly to high-frequency noise from the tail current source stage, the proposed noise reduction technique reduces only the white noise of the load resistor mixed with a DC component of switching.

Fig. 4 shows the common-mode feedback scheme for white noise introduced by the load resistor. The output white voltage noise can be defined as follows:

$$\overline{V^2_{o+,RL+}} = \left(\frac{1+g_{mcs}R_L/2}{1+g_{mcs}R_L}\right)^2 R_L^2 \cdot \overline{i^2_{n,RL+}} \tag{11a}$$

$$\overline{V^2_{o-,RL+}} = \left(\frac{g_{mcs}R_L/2}{1+g_{mcs}R_L}\right)^2 R_L^2 \cdot \overline{i^2_{n,RL+}} \tag{11b}$$

Comparing (10) and (11) indicates that the common-mode feedback decreases the output white noise for $V_{\mathrm{o+,RL+}}$ but newly produces $V_{\mathrm{o-,RL+}}$.

In summary, because the tail current source and RF transconductance stages consist of two transistors each, the switching stage has four transistors, and the load stage has two resistors, the total output white voltage noise at the single output port in the conventional mixer can be represented as

$$\overline{V^2_{o\pm,wn}} = \frac{R_L^2 \cdot \overline{i^2_{wn,CS+}}}{2} + \left[ (1-a)^2 + \left(\frac{2}{\pi}\right)^2 (1+a)^2 \right] \times \frac{R_L^2}{2} \cdot \overline{i^2_{wn,RF+}} + 4R_L^2 \cdot \overline{i^2_{wn,sw+}} + R_L^2 \cdot \overline{i^2_{n,RL+}} \tag{12}$$

**TABLE 1. Single-ended output noise power from each noise contributor.**

| | Conventional Mixer (dBm/Hz) | | Proposed Mixer (dBm/Hz) | | Noise Reduction (dB) | |
|---|---|---|---|---|---|---|
| | Cal. | Sim. | Cal. | Sim. | Cal. | Sim. |
| **Low-frequency noise at 10 kHz** | | | | | | |
| Current source stage ($M_1$, $M_2$) | −141.1 | −143.5 | −162.4 | −164.2 | 21.3 | 20.7 |
| Transconductance stage ($M_3$, $M_4$) | −144.5 | −147.5 | −160.6 | −161.4 | 16.1 | 13.9 |
| LO switching stage ($M_5$–$M_8$) | −151.6 | −154.2 | −151.6 | −155.5 | — | — |
| Load stage ($R_L$) | −156 | −157.6 | −159 | −163.3 | 3 | 5.7 |
| DC level shifter ($M_9$–$M_{12}$) | — | — | −166.9 | −167.1 | — | — |
| Current bleeding stage($M_{13}$) | — | −164.8 | — | −173.5 | — | 8.7 |
| Output buffer | −160.2 | −162.5 | −160.2 | −162.5 | — | — |
| Other sources | — | −161.9 | — | −170.8 | — | — |
| Total | −139.1 | −142.7 | −147.8 | −153.5 | 9.7 | 10.8 |
| DSB NF (dB) | 19.2 | 19.9 | 9.5 | 9.1 | 9.7 | 10.8 |
| **High-frequency noise at 100 MHz** | | | | | | |
| Current source stage ($M_1$, $M_2$) | −152.0 | −153.2 | −173.3 | −172.8 | 21.3 | 19.6 |
| Transconductance stage ($M_3$, $M_4$) | −160.8 | −161.0 | −161.8 | −162.2 | 1 | 1.2 |
| LO switching stage ($M_5 - M_8$) | −169.8 | −170.6 | −169.8 | −171.4 | — | — |
| Load stage ($R_L$) | −157.8 | −158.3 | −160. | −161.3 | 2.2 | 3 |
| DC level shifter ($M_9 - M_{12}$) | — | — | −172.6 | −179.6 | — | — |
| Current bleeding stage($M_{13}$) | — | −175.5 | — | −185.6 | — | 10.1 |
| Output buffer | −170.3 | −171.8 | −170.3 | −174.7 | — | — |
| Other sources | — | −163.6 | — | −166.7 | — | — |
| Total | −150.4 | −153.9 | −155.7 | −158.7 | 5.3 | 4.8 |
| DSB NF (dB) | 11.0 | 9.7 | 5.68 | 4.9 | 5.3 | 4.8 |

Note: results listed are for $g_{mcs}$ = 13.3 mS, $g_{mRF}$ = 12.25 mS, $g_{mLO}$ = 6.8 mS, $r_{o,cs}$=164 Ω, $r_{o,RF}$ = 1.7 kΩ, $R_L$ = 1000 Ω, $I$ = 0.27 mA, and $A$ = 0.52 V.

In the proposed mixer, the total output white voltage noise at the single output port can be expressed as

$$\begin{aligned}\overline{V_{o\pm,wn}^2} = {} & \frac{R_L^2/2}{(1+g_{mcs}R_L)^2}\cdot\overline{i_{wn,CS+}^2}+ \\ & +\left[\frac{(1-a)^2}{(1+g_{mcs}R_L/2)^2}+\left(\frac{2}{\pi}\right)^2(1+a)^2\right] \\ & \times\frac{R_L^2}{2}\cdot\overline{i_{wn,RF+}^2}+4R_L^2\cdot\overline{i_{wn,sw+}^2} \\ & +\left[\left(\frac{1+g_{mcs}R_L/2}{1+g_{mcs}R_L}\right)^2+\left(\frac{g_{mcs}R_L/2}{1+g_{mcs}R_L}\right)^2\right] \\ & \times R_L^2\cdot\overline{i_{n,RL+}^2}. \end{aligned} \tag{13}$$

A large noise-reduction in the proposed mixer can be obtained by increasing the feedback factors $g_{mcs}$ and $R_L$. However, implementing such increases in the proposed mixer involves various tradeoffs; for example, to achieve a large $g_{mcs}$, the size or current of the tail current transistor needs to be increased. The large transistor needs to decrease the overdrive voltage for low current consumption, but it is limited by the threshold voltage. In addition, the large current increases power consumption and the switching noise in (4) and needs to decrease $R_L$ under the voltage-constrained condition, which results in low conversion gain. Nevertheless, if $R_L$ is increased to obtain a large feedback factor, the voltage headroom is issued. Therefore, the proposed mixer in Fig. 1 is appropriately designed with the transistor length ($L$) of 0.2 $\mu$m, transistor widths of $M_{1,2}$ ($W_{1,2}$) of 240 μm, $W_{3,4}$ of 48 μm, $W_{5-8}$ of 300 μm, $W_{9-12}$ of 200 μm, $W_{13}$ of 250 μm, $R_L$ of 1 kΩ, $V_{DD}$ of 1.5 V, and total current consumption of 2.2 mA, including 0.2 mA by the DC level shifter.

## III. VALIDATION OF THEORY BY SIMULATION

To validate the theoretical analysis, we simulated the output noise appearing at the single output port of the conventional and proposed mixers using a Cadence tool. The noise at the single output port is a total noise consisted of the common-mode noise and the differential-mode noise. The conventional mixer was configured with the same circuit as in the proposed mixer except the DC level shifter. Both mixers are designed for the same power consumption, conversion gain, and linearity performances.

Table 1 lists noise contributions (with respect to 50 Ω) at low frequency (10 kHz) and a high frequency (100 MHz) ranges from the current source, transconductance, switching, load, DC level shifter, output buffer stages, and other sources; the other sources include 50-Ω port input ($R_s$) and output ($R_o$) resistors, gate-bias resistors, and parasitic resistances of passive components, each of which weakly contributes to the total noise. The calculation is based on the theoretical analysis in the previous section except the DC level shifter and output buffer. Noise current from the DC level shifter can be converted to that of the tail current source by multiplying $((r_{o9}//r_{o11}//1/g_{m9})\times g_{m1})^2$ to (3a) and (8a) for the low- and high-frequency noise calculations, respectively. The output buffer is configured with a $p$MOS common-source amplifier with a 50-Ω load resistor ($R_B$). Noise current from the buffer stage is multiplied by $(R_B//R_o)^2/R_o$ to obtain output noise power.

The input-referred flicker noise voltage density of a MOSFET is

$$\overline{V_{fn}^2} = \frac{K}{C_{ox}WL}\cdot\frac{1}{f} \tag{14}$$

where $K$ is a process-dependent constant, and $C_{ox}$ is the gate-oxide capacitance. Note that the values of $K$ and $\gamma$ in (7) and (9) were approximately extracted from regular noise simulations of MOSFETs and documents offered by the foundry

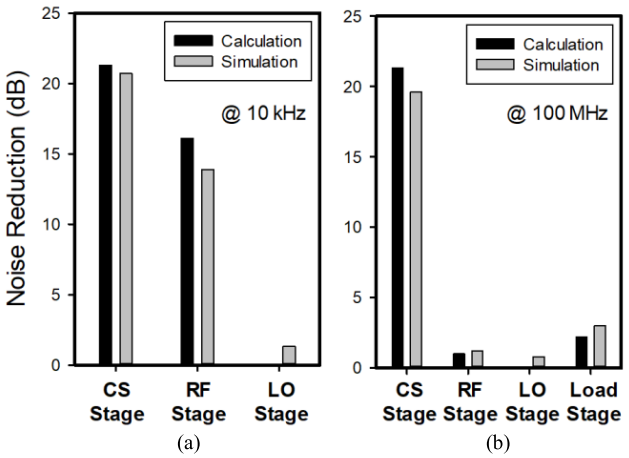


**FIGURE 5.** Noise reduction of the main noise contributors at (a) low frequency (10 kHz) and (b) high frequency (100 MHz).

provider. The double-side-band noise figure (DSB NF) can be expressed as

$$DSB\,NF = 10\log\left(\frac{1}{2}\frac{\overline{V_{o+}^2}}{A_v^2 4kTR_s}\right) \tag{15a}$$

where

$$A_v = \frac{1}{\pi} g_{mrf} R_L \tag{15b}$$

Here, $V_{o+}$ is the single output voltage noise, and $A_v$ is the conversion gain from the single source voltage to the single output voltage.

Regarding the low-frequency noise of the conventional mixer, we recognize from Table 1 that the main noise source is the tail current source stage. In the proposed mixer, this noise and flicker noise from the transconductance stage are strongly reduced by the common-mode feedback, based on (3). Flicker noise from the switching stage is, however, not reduced due to the differential output noise, based on (4). The output buffer's flicker noise becomes dominant in the proposed mixer because it is out of the feedback loop and thus not reduced by the feedback. However, it can be ignored because the output buffer is generally not used when the IF amplifier, which has high input impedance, is followed in integrated circuits.

Regarding the high-frequency noise of the conventional mixer, the main noise source is the transconductance stage. In the proposed mixer, the output white noise from that stage is rarely reduced by the common-mode feedback because it mostly consists of the differential output described by (8b). Meanwhile, output white noise from the tail current source stage is strongly reduced, as described by (8a). White noise from the load stage is somewhat reduced, as described by (11).

Fig. 5 shows the noise reductions for the main noise contributors at low and high frequencies. The low-frequency noise is mainly generated by the current source stage. In the situation shown in Fig. 5(a), it is very important to obtain a large noise reduction of approximately 21 dB by the proposed feedback technique. In addition, the low-frequency noise from the transconductance stage is reduced by approximately 14 dB. As a result, the common-mode feedback reduces the total output flicker noise and also DSB NF by approximately 10.8 dB. As shown in Fig. 5(b), the high-frequency noises from the tail current source and load stages partly contribute to the total noise and are reduced by approximately 20 and 3 dB, respectively. Because the high-frequency noise from the transconductance stage mostly consists of differential-mode noise, there is little noise reduction by the common-mode feedback described in (8b). For the switching stage at low and high frequencies, there is no calculated noise reduction due to neglect of the channel-length modulation effect in (4) and (9). As a result, the proposed feedback technique reduces the total white noise by approximately 5 dB.

In summary, the proposed common-mode feedback technique is a simple method to enhance the noise performance of mixers. All calculations and simulations at low and high frequencies were well matched. Therefore, the theoretical analysis was well validated by the simulation.

## IV. EXPERIMENTAL RESULTS

To verify the proposed noise reduction technique, the conventional and proposed mixers were fabricated using a 65 nm RF CMOS process. A microphotograph of the proposed mixer is given in Fig. 6. The chip size including the pads was 0.94 $mm^2$. All measurements were performed using on-wafer probing, with a signal generator (Agilent E8257C) at the RF input and a signal analyzer (Agilent N9030A) at the IF output. All off-chip losses in the cables, baluns, and DC-blocking capacitors were de-embedded from the measurement results. The total bias current consumed 2.3 mA with a supply voltage of 1.5 V.

Fig. 7 illustrates the calculated, simulated, and measured single-port DSB NFs for conventional and proposed mixers with an LO power of −4 dBm at an LO frequency of 2 GHz. The calculated results were obtained by extrapolation and summation of flicker noise (−10 dB/decade) at 1 kHz and white noise at 100 MHz. The single-port DSB NF was measured using the gain method [16]. The measured NFs of the conventional and proposed mixers were 22.5 and 12.5 dB at 10 kHz and 10.3 and 6.9 dB at 100 MHz, respectively. As a result, the measured noise reduction was 10.0 and 3.4 dB below and above the corner frequency of hundreds of kHz, respectively. Fig. 8 shows the simulated and measured DSB NFs versus the RF input frequency for both mixers at an IF frequency of 100 MHz. Note that the proposed feedback technique works well at wide bandwidth because the feedback path from the IF output to the tail current source stage does not affect the RF signals.

Fig. 9 shows the simulated and measured conversion gains versus RF input frequency. The measured conversion gains of the conventional and proposed mixers were 20.2 and 21.5 dB, respectively. A two-tone test of the proposed mixer with a

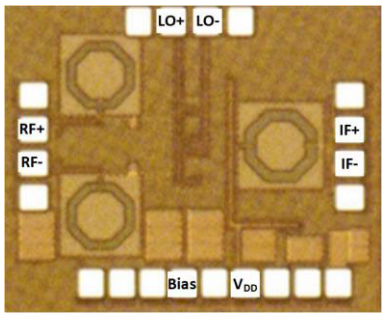


**FIGURE 6.** The microphotograph of the proposed mixer.

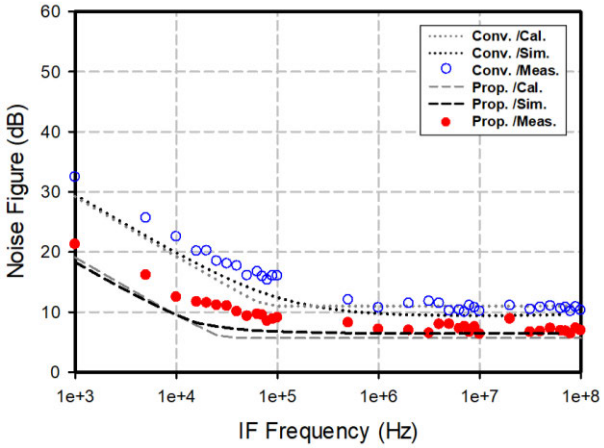


**FIGURE 7.** Calculated, simulated, and measured single-port DSB NFs for conventional and proposed mixers at an LO frequency of 2 GHz.

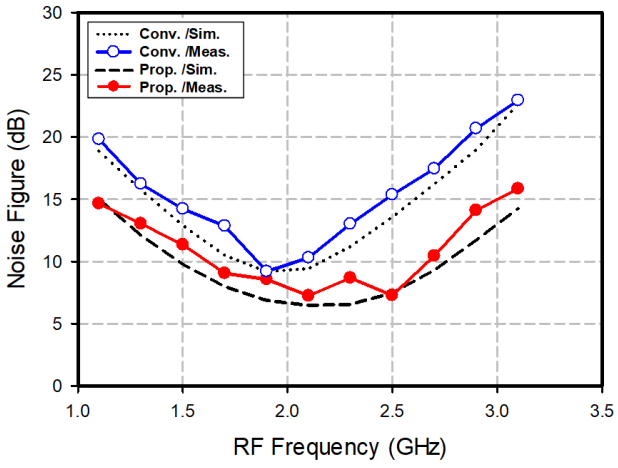


**FIGURE 8.** Simulated and measured single-port DSB NFs versus RF input frequency for conventional and proposed mixers at an IF of 100 MHz.

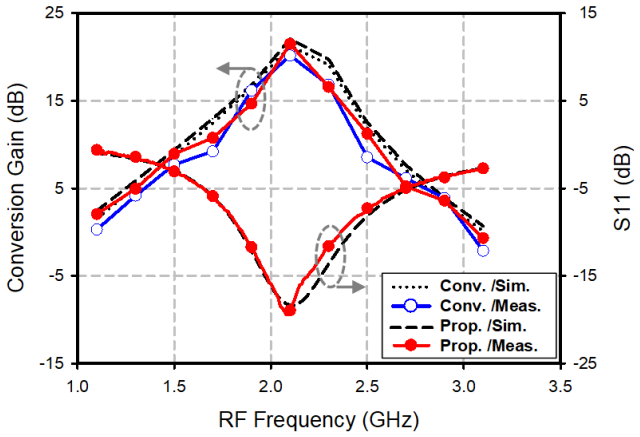


**FIGURE 9.** Simulated and measured conversion gains and S11 versus RF input frequency for conventional and proposed mixers at an IF of 100 MHz.

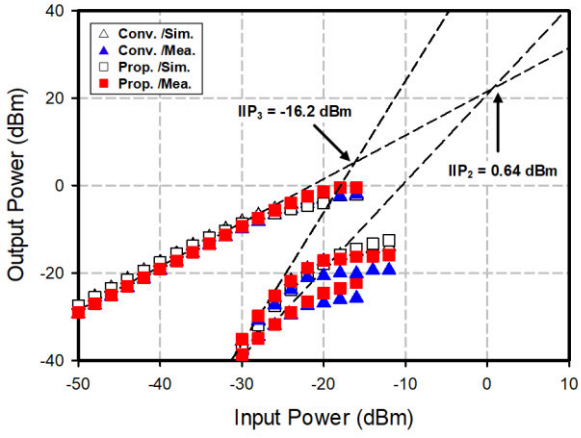


**FIGURE 10.** Simulated and measured P1dB, IIP2, and IIP3 for the conventional and proposed mixers.

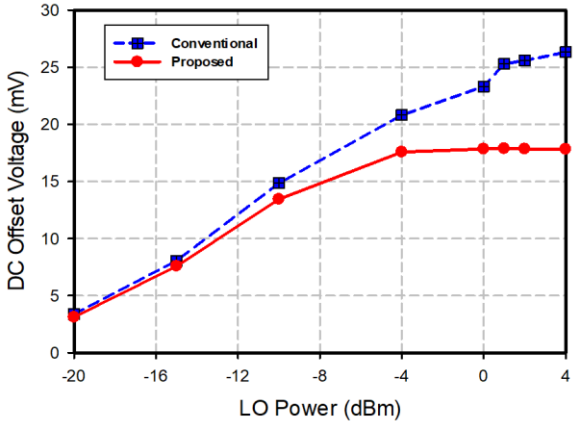


**FIGURE 11.** Measured DC offset voltage from LO self-mixing versus LO power for the conventional and proposed mixers.

frequency spacing of 50 MHz showed a P1dB of −25.7 dBm, an IIP2 of 0.64 dBm, and an IIP3 of −16.2 dBm in Fig. 10. The proposed mixer design focuses on achieving low noise performance. In order to lower noise figure, a higher gain is required as shown in (15a), which leads to decrease in IIP3.

The DC offset voltage is measured, as shown in Fig. 11, which demonstrates that the proposed mixer improves the

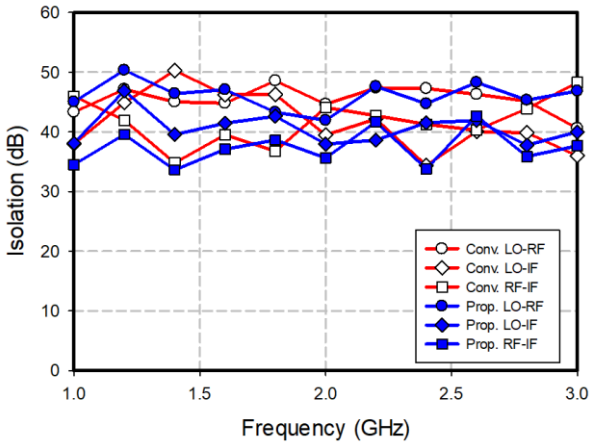


**FIGURE 12.** Measured port-to-port isolation of the conventional and proposed mixers.

**TABLE 2.** Performance comparisons of conventional and proposed mixers.

| | Tech. (nm) | RF freq. (GHz) | DSB NF (dB) (1) @ 10 kHz | DSB NF (dB) (1) @ 100 MHz | CG (dB) | IIP3 (dBm) | $P_{DC}$ (mW) |
|---|---|---|---|---|---|---|---|
| Conv. Mixer | 65 | 2.1 | 22.5 | 10.3 | 20.2 | -14.95 | 3.15 |
| Prop. Mixer | 65 | 2.1 | 12.5 | 6.9 | 21.5 | -16.2 | 3.45(2) |

(1) single-port noise figure, (2) including feedback circuit power dissipation

DC offset performance, compared to the conventional mixer, as described previously. The conventional and proposed mixers have a good port-to-port isolation characteristic of greater than 33 dB, as shown in Fig. 12. The measured results are summarized in Table 2. The conversion gain and IIP3 of the proposed and conventional mixers are slightly different due to the loading effect of the common-mode feedback circuit.

## V. PVT ROBUSTNESS AND DISCUSSION

### A. PROCESS-VOLTAGE-TEMPERATURE VARIATION

The proposed common-mode feedback technique is a type of negative feedback with PVT robustness, which is described in detail in this section. Because mismatch and process variations convert common-mode noise into differential-mode noise, the differential DSB NF is the main focus in this section.

Fig. 13 presents process corner simulations and measurements of 42 samples for the differential DSB NF. Using the proposed feedback technique, the proposed mixer obtained smaller fluctuations of NF in corner simulation and measurement than the conventional mixer. The measured data are distributed due to chip-to-chip process variations and measurement errors. Although on-wafer probing is adopted for this differential NF measurement of many chips, which produces measurement errors due to sensitivity to probe

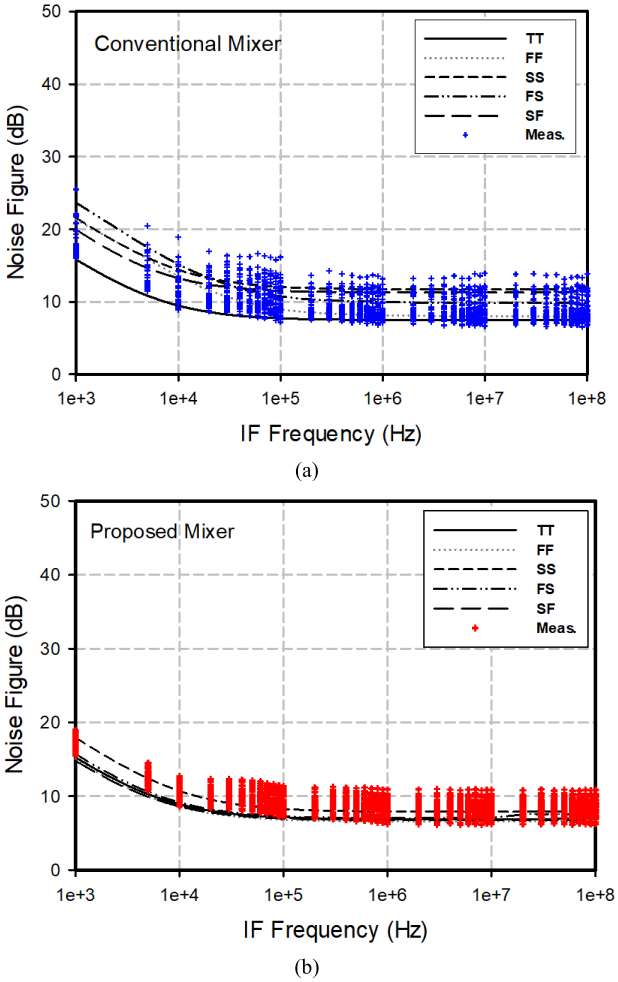


**FIGURE 13.** Simulated and measured differential DSB NF of the (a) conventional and (b) proposed mixers, with process corners (TT FF SS FS SF) and 42 samples.

touch-down. Nevertheless, the measured result is very similar to the simulated one in trend.

Figs. 14 and 15 illustrate Monte Carlo simulations with 200 iterations over the process variations and mismatch and measurements with 42 samples, respectively, for both mixers' differential NF at 10 kHz in order to demonstrate one of the benefits of the proposed common-mode feedback technique. Figs. 14(a) and 15(a) show a wide spread of NF arising from the mismatch and process variations. As shown in Figs. 14(b) and 15(b), the proposed feedback technique results in higher yield in NF with a smaller mean ($\mu$) and standard deviation ($\sigma$) compared to the conventional mixer. In addition, if the voltage and temperature variations are considered, the NF performance is further degraded for the conventional mixer in Fig. 14(a), whereas the proposed mixer presents more stable noise performance in Fig. 16(b) due to the negative feedback structure. The proposed mixer also achieves robustness of conversion gain and third-order input intercept point (IIP3) for the PVT variations, which are not illustrated in detail.

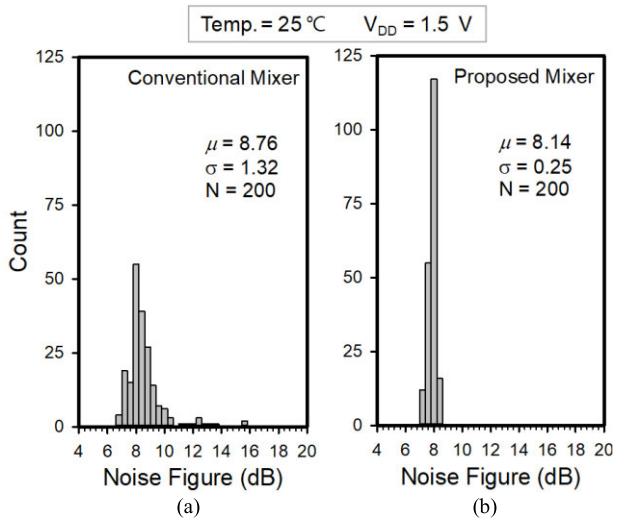


**FIGURE 14.** Monte Carlo simulation of process variation and mismatch for differential NF at 10 kHz in the (a) conventional and (b) proposed mixers.

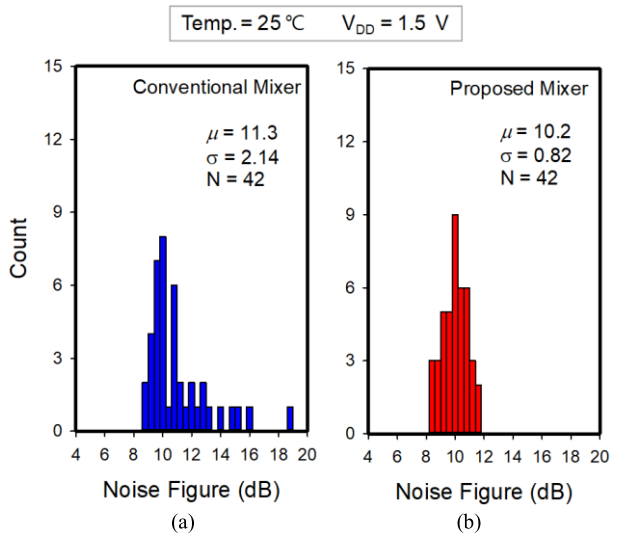


**FIGURE 15.** Measured differential NF at 10 kHz for the (a) conventional and (b) proposed mixers with 42 samples.

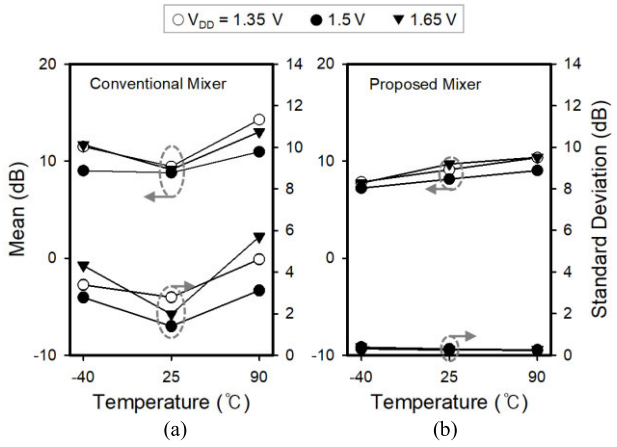


**FIGURE 16.** Mean ($\mu$) and standard deviation ($\sigma$) of differential NF at 10 kHz over the PVT variations for (a) conventional and (b) proposed mixers.

In Table 3, the proposed mixer performances are summarized and compared with state-of-the-art low-flicker-noise

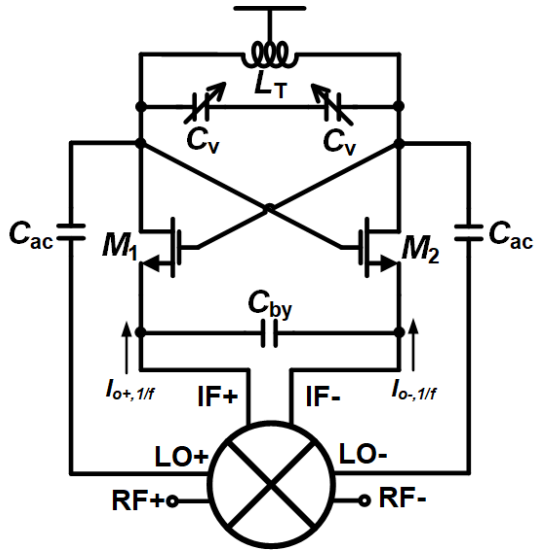


**FIGURE 17.** Schematic of the self-oscillating mixer (SOM) consisting of the proposed mixer and a typical cross-coupled LC-tank VCO.

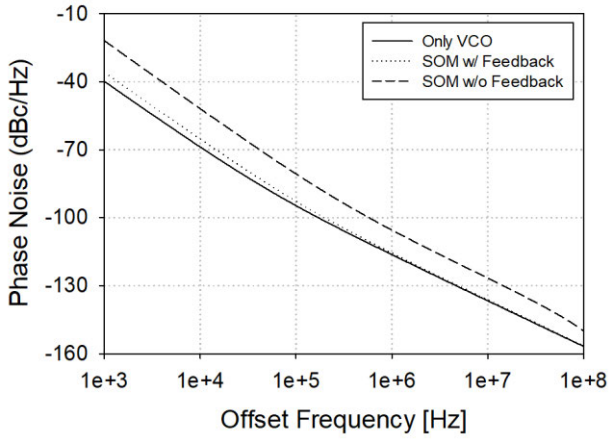


**FIGURE 18.** Simulated phase noise for a VCO only and two SOMs with and without feedback.

CMOS mixers [11], [17], [18], [19], [20], [21], [22], [23], [24]. The proposed mixer with feedback achieved an excellent figure-of-merit (FOM).

### B. DISCUSSION OF COMMON-MODE NOISE EFFECT ON SOM

As described in Introduction, the common flicker noise of the mixer degrades the phase noise of the VCO in a self-oscillating mixer (SOM) [12]; this is because the common flicker noise flowing into the VCO increases the AM-to-PM noise. Fig. 17 shows an SOM composed of the proposed mixer with a current-reuse VCO. The VCO consists of a cross-coupled nMOS pair, an inductor ($L_T$), a varactor ($C_v$), an AC-coupling capacitor ($C_{ac}$), and a bypass capacitor ($C_{by}$). Fig. 18 shows the simulated phase noise performances for a VCO only as well as for two SOMs with and without common-mode feedback. The VCO in the SOM

**TABLE 3. Performance summary and comparison to low-noise CMOS mixers.**

| Reference | Process (μm) | RF freq. (GHz) | DSB NF (dB) @ 10 kHz | DSB NF (dB) @ 100 MHz | CG (dB) | 3-dB BW (GHz) | IIP3 (dBm) | $V_{DD}$ (V) | $P_{DC}$ (mW) | FOM1[(1)] (dB) | FOM2[(2)] (dB) |
|---|---|---|---|---|---|---|---|---|---|---|---|
| [11] | 0.11 | 2.4 | 14.2[(4)] | 5.1[(4)] | 19[(5)] | 2.5 | -7 | 1.3 | 3[(4)] | 20.5[(4)(5)] | 17[(4)(5)] |
| [17] | 0.13 | 2.1 | 8.2[(4)] | 3.9[(4)] | 24.1 | 0.7 | -14.5 | 1.2 | 2.1[(4)] | 42.7[(4)] | 28.2[(4)] |
| [18] | 0.13 | 5 | - | 4.2 | 15 | 5.3 | 2.5[(8)] | 1.5 | 25.5 | - | - |
| [19] | 0.18 | 1 | 25[(3)] | 11.4 | 12.9 | - | 3.6 | 1.8 | 3.3 | 12.7 | 16.3 |
| [20] | 0.13 | 2.4 | 26[(3)] | 7.2 | 22[(5)(7)] | 0.7 | 16[(8)] | 1.2 | 3.15[(7)] | 10[(5)(7)] | 18[(5)(7)(8)] |
| [21] | 0.13 | 0.9 | 24.8[(3)] | 8.5 | 18.4 | - | 12.5[(8)] | 1 | 4.0 | 17.6 | 30.1[(8)] |
| [22] | 0.065 | 2.4 | 21.5[(3)] | 3.9 | 11.2 | - | 6.7 | 1.2 | 8.4 | 10.5 | 17.2 |
| [23] | 0.065 | 2.4 | 22[(3)] | 10.5 | 12.5[(5)] | 0.2 | 7.6[(8)] | 1 | 1.2 | 13.5[(5)] | 17.3[(5)(8)] |
| [24] | 0.065 | 2.4 | 9.17 | 7.23 | 14.6[(5)] | 0.4 | -15.89 | 1.5 | 3.82 | 22.31[(5)] | 14.4[(5)] |
| **This work** | **0.065** | **2.1** | **8.7** | **7.1** | **21.5** | **0.4** | **-16.2** | **1.5** | **3.45** | **37.4** | **21.2** |

[(1)] FOM1 (dB) = CG – NF@10 kHz – $P_{DC}$; [(2)] FOM2 (dB) = CG + IIP3 – NF@10 kHz – $P_{DC}$; [(3)] extrapolation; [(4)] single-balanced mixer; [(5)] voltage conversion gain;[(6)] excluding auxiliary circuit power; [(7)] LNA+Mixer; [(8)] using a linearity improvement technique

with feedback showed superior phase noise performance compared to the one without feedback; this is because the common flicker noise was reduced by the common-mode feedback. The VCO in the SOM with feedback was somewhat noisier than the VCO only since the common-mode flicker noise in the proposed mixer was still present due to the insufficient amount of feedback. Therefore, it is important to reduce the common noise in the mixer for high-performance transceivers.

## VI. CONCLUSION

The proposed common-mode feedback for CMOS mixers suppresses common-mode flicker and white noise without degrading other performances. Noise analysis based on the negative feedback theory was performed for low- and high-frequency noise and was validated by simulation and measurement. As an advantage of the common-mode feedback, the proposed mixer reduced common-mode noise and sensitivity to PVT variations. In addition, the proposed feedback technique was very effective in conjunction with other low noise techniques and improved the phase noise performance in SOM. Therefore, the proposed common-mode feedback technique can be usefully applied to various active mixers.

## ACKNOWLEDGMENT

The MPW and software tools were supported by the IC Design Education Center (IDEC), South Korea.

## REFERENCES

[1] B. Razavi, *RF Microelectronics*. Upper Saddle River, NJ, USA: Prentice-Hall, 1998.

[2] H. Darabi and A. A. Abidi, "Noise in RF-CMOS mixers: A simple physical model," *IEEE J. Solid-State Circuits*, vol. 35, no. 1, pp. 15–25, Jan. 2000.

[3] L. A. NacEachern and T. Manku, "A charge-injection method for Gilbert cell biasing," in *Proc. IEEE Can. Conf. Electr. Comput. Eng.*, vol. 1, May 1998, pp. 365–368.

[4] J. Park, C.-H. Lee, B.-S. Kim, and J. Laskar, "Design and analysis of low flicker-noise CMOS mixers for direct-conversion receivers," *IEEE Trans. Microw. Theory Techn.*, vol. 54, no. 12, pp. 4372–4380, Dec. 2006.

[5] C.-R. Wu, H.-H. Hsieh, and L.-H. Lu, "An ultra-wideband distributed active mixer MMIC in 0.18-$\mu$m CMOS technology," *IEEE Trans. Microw. Theory Techn.*, vol. 55, no. 4, pp. 625–632, Apr. 2007.

[6] S. Kong, C.-Y. Kim, and S. Hong, "A K-band UWB low-noise CMOS mixer with bleeding path $G_m$-boosting technique," *IEEE Trans. Circuits Syst. II, Exp. Briefs*, vol. 60, no. 3, pp. 117–121, Mar. 2013.

[7] H. Darabi and J. Chiu, "A noise cancellation technique in active RF-CMOS mixers," *IEEE J. Solid-State Circuits*, vol. 40, no. 12, pp. 2628–2632, Dec. 2005.

[8] J. Yoon, H. Kim, C. Park, J. Yang, H. Song, S. Lee, and B. Kim, "A new RF CMOS Gilbert mixer with improved noise figure and linearity," *IEEE Trans. Microw. Theory Techn.*, vol. 56, no. 3, pp. 626–631, Mar. 2008.

[9] C.-H. Chen, P.-Y. Chiang, and C. F. Jou, "A low voltage mixer with improved noise figure," *IEEE Microw. Wireless Compon. Lett.*, vol. 19, no. 2, pp. 92–94, Feb. 2009.

[10] M. Rahman and R. Harjani, "A sub-1-V 194-$\mu$W 31-dB FOM 2.3–2.5 GHz mixer-first receiver frontend for WBAN with mutual noise cancellation," *IEEE Trans. Microw. Theory Techn.*, vol. 64, no. 4, pp. 1102–1109, Apr. 2016.

[11] J. Lee, J. Park, and T. Yun, "Flicker noise improved CMOS mixer using feedback current bleeding," *IEEE Microw. Wireless Compon. Lett.*, vol. 27, no. 8, pp. 730–732, Aug. 2017.

[12] A. Liscidini, A. Mazzanti, R. Tonietto, L. Vandi, P. Andreani, and R. Castello, "Single-stage low-power quadrature RF receiver front-end: The LMV cell," *IEEE J. Solid-State Circuits*, vol. 41, no. 12, pp. 2832–2841, Dec. 2006.

[13] W. Kim, S.-G. Yang, J. Yu, H. Shin, W. Choo, and B.-H. Park, "A direct conversion receiver with an IP2 calibrator for CDMA/PCS/GPS/AMPS applications," *IEEE J. Solid-State Circuits*, vol. 41, no. 7, pp. 1535–1541, Jul. 2006.

[14] J.-H. Kim, H.-W. An, and T.-Y. Yun, "A low-noise WLAN mixer using switched biasing technique," *IEEE Microw. Wireless Compon. Lett.*, vol. 19, no. 10, pp. 650–652, Oct. 2009.

[15] M.-G. Kim, H.-W. An, Y.-M. Kang, J.-Y. Lee, and T.-Y. Yun, "A low-voltage, low-power, and low-noise UWB mixer using bulk-injection and switched biasing techniques," *IEEE Trans. Microw. Theory Techn.*, vol. 60, no. 8, pp. 2486–2493, Aug. 2012.

[16] Maxim Integrated Products. *Three Methods of Noise Figure Measurement AN2875*. Accessed: Jul. 5, 2021. [Online]. Available: https://www.maximintegrated.com

[17] J.-Y. Lee and T.-Y. Yun, "Low-flicker-noise and high-gain mixer using a dynamic current-bleeding technique," *IEEE Microw. Wireless Compon. Lett.*, vol. 27, no. 8, pp. 733–735, Aug. 2017.

[18] B. Guo, H. Wang, and G. Yang, "A wideband merged CMOS active mixer exploiting noise cancellation and linearity enhancement," *IEEE Trans. Microw. Theory Techn.*, vol. 62, no. 9, pp. 2084–2091, Sep. 2014.
[19] B. Guo, J. Gong, Y. Wang, C. Liu, L. Li, J. Wu, and H. Liu, "Low-frequency noise in CMOS switched-gm mixers: A quasi-analytical model," *IEEE Access*, vol. 8, pp. 191219–191230, 2020.
[20] N. Vitee, H. Ramiah, P. Mak, J. Yin, and R. P. Martins, "A 3.15-mW +16.0-dBm IIP3 22-dB CG inductively source degenerated balun-LNA mixer with integrated transformer-based gate inductor and IM2 injection technique," *IEEE Trans. Very Large Scale Integr. (VLSI) Syst.*, vol. 28, no. 3, pp. 700–713, Mar. 2020.
[21] N. Vitee, H. Ramiah, P. Mak, J. Yin, and R. P. Martins, "A 1-V 4-mW differential-folded mixer with common-gate transconductor using multiple feedback achieving 18.4-dB conversion gain, +12.5-dBm IIP3, and 8.5-dB NF," *IEEE Trans. Very Large Scale Integr. (VLSI) Syst.*, vol. 28, no. 5, pp. 1164–1174, May 2020.
[22] B. Guo and J. Gong, "A dual-band low-noise CMOS switched-transconductance mixer with current-source switch driven by sinusoidal LO signals," in *Proc. IEEE Int. Midwest Symp. Circuits Syst. (MWSCAS)*, Aug. 2021, pp. 741–744.
[23] M. H. Kashani, M. Asghari, M. Yavari, and S. Mirabbasi, "A +7.6 dBm IIP3 2.4-GHz double-balanced mixer with 10.5 dB NF in 65-nm CMOS," *IEEE Trans. Circuits Syst. II, Exp. Briefs*, vol. 68, no. 10, pp. 3214–3218, Oct. 2021.
[24] S. Pang, Y. Kim, and T. Yun, "High-gain, low-power, and low-noise CMOS mixer using current-reused bleeding amplification," *IEEE Microw. Wireless Compon. Lett.*, vol. 32, no. 5, pp. 418–421, May 2022.

**CHANG-WOO LIM** received the B.S. degree in electronics computer engineering from Hanyang University, Seoul, South Korea, in 2011, where he is currently pursuing the Ph.D. degree with the Department of Electronics Engineering. His research interests include RF integrated circuits and systems for wireless applications.

**JI-YOUNG LEE** received the B.S. degree in electronic and electrical engineering from Hongik University, Seoul, South Korea, in 2010, and the Ph.D. degree from the Department of Electronics Engineering, Hanyang University, Seoul, in 2017. Since 2017, he has been an NAND Flash Memory Circuit Design Engineer with SK Hynix Inc., Icheon, South Korea. His research interests include SI, PI, and high-speed interface systems.

**MYOUNG-GYUN KIM** received the B.S. and M.S. degrees in electronics computer engineering from Hanyang University, Seoul, Republic of Korea, in 2007 and 2009, respectively, and the Ph.D. degree from the Department of Electronics Engineering, Hanyang University. He is currently with Samsung Electronics Company Ltd., Hwaseong-si, Gyeonggi-do, South Korea. His research interests include CMOS RFIC and systems design for wireless applications.

**TAE-YEOUL YUN** (Member, IEEE) received the Ph.D. degree from the Department of Electrical Engineering, Texas A&M University, College Station, TX, USA, in 2001. From 1989 to 1996, he was with the Optical Telecommunication System Group, ETRI, Daejeon, South Korea, where he developed 2.5- and 10-Gb/s systems. From 2001 to 2003, he was an MMIC Designer with Triquint Semiconductor, Dallas, TX, USA. Since 2003, he has been a Professor with Hanyang University, Seoul, South Korea. His research interests include RFICs, antennas, and wireless/optical high-speed communication systems.